

# Stereoengineering of Poly(1,3-methylenecyclohexane) via Two-State Living Coordination Polymerization of 1,6-Heptadiene

Kaitlyn E. Crawford and Lawrence R. Sita\*

Department of Chemistry and Biochemistry, University of Maryland, College Park, Maryland 20742, United States

**S** Supporting Information

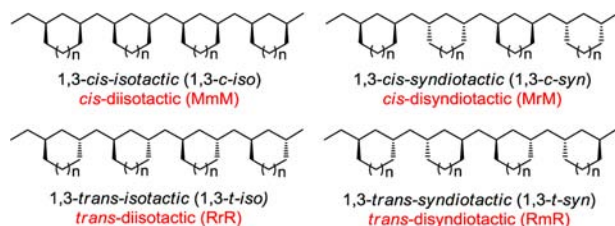
**ABSTRACT:** External control over the rate of dynamic methyl group exchange between configurationally stable active species and configurationally unstable dormant species with respect to chain-growth propagation within a highly stereoselective and regiospecific living coordination polymerization of 1,6-heptadiene has been used to generate a spectrum of different physical forms of poly(1,3-methylenecyclohexane) (PMCH) in which the stereochemical microstructure has been systematically varied between two limiting forms. The application of this strategy to manipulate the bulk properties of PMCH and the solid-state microphase behavior of well-defined PMCH-*b*-poly(1-hexene) block copolymers is further demonstrated.

Since the mid-1990s, advances made with the discovery of molecularly discrete transition-metal complexes that can serve as initiators for the (stereoselective) living coordination polymerization (LCP) of olefins have brought the long-sought-after goal of obtaining “precision” polyolefins with unique polymer architectures and physical properties closer to reality.<sup>1,2</sup> One major drawback often encountered in the development of polyolefin-based structural materials, however, is a low glass transition temperature ( $T_g$ ) that is associated with a linear, acyclic polymer framework (e.g.,  $T_g$  of ca.  $-100$  and  $-15$  °C for polyethylene and *isotactic* polypropene, respectively, vs ca.  $100$  °C for polystyrene).<sup>3</sup> Restriction of chain conformational mobility through incorporation of sterically encumbered side chains has been shown to be an effective strategy for increasing  $T_g$ , but the evolution of crystallinity coupled with either a high melting temperature ( $T_m$ ), complex crystallization kinetics, or the coexistence of different crystal forms can also be deleterious.<sup>4</sup> As shown in Chart 1, poly(1,3-methylenecycloalkane)s (PMCA), as derived from the coordination polymerization of  $\alpha,\omega$ -nonconjugated dienes, are more structurally and stereo-

chemically diverse than linear poly( $\alpha$ -olefins).<sup>5–11</sup> In this respect, we have previously shown that the class of soluble cationic group 4 metal complexes having the general formula  $\{(\eta^5\text{-C}_5\text{R}_5)\text{M}[\text{N}(\text{R}^1)\text{C}(\text{R}^2)\text{N}(\text{R}^3)](\text{Me})\}[\text{B}(\text{C}_6\text{F}_5)_4]$  ( $\text{M} = \text{Zr}, \text{Hf}$ ), which are generated in situ through “activation” of the neutral dimethyl precursor  $\{(\eta^5\text{-C}_5\text{R}_5)\text{M}[\text{N}(\text{R}^1)\text{C}(\text{R}^2)\text{N}(\text{R}^3)](\text{Me})_2$  (**I**) using 1 equiv of  $[\text{PhNHMe}_2][\text{B}(\text{C}_6\text{F}_5)_4]$  (**II**), are effective initiators for the (stereoselective) LCP of ethene, propene, and related olefins to provide polyolefins possessing narrow molecular weight distributions and tunable degrees of polymerization.<sup>2,12</sup> In the case of 1,5-hexadiene (1,5-HXD), the corresponding poly(1,3-methylenecyclopentane) (PMCP;  $n = 0$  in Chart 1) was also incorporated into PMCP-*b*-poly( $\alpha$ -olefin) block copolymers that were shown to adopt solid-state, long-range-ordered microphase-separated morphologies with feature sizes on the nanometer length scale.<sup>8</sup> On the other hand, these PMCP materials were still characterized by a low  $T_g$  of  $-12$  °C and a  $T_m$  of  $94$  °C. Further, even after an empirical evaluation of several different derivatives of **I**, the inability to improve upon both poor 1,3-*cis*/1,3-*trans* stereoselectivity and less-than-ideal regioselectivity for ring-closing insertion during chain-growth propagation, which generates a low level ( $\sim 1$ – $2\%$ ) of undesirable reactive pendant vinyl groups, has hindered our efforts to develop more complex polymer architectures and extensive material science surrounding these PMCP-based polyolefins. Herein, we report the extension of these investigations to include the stereoselective and regiospecific LCP of 1,6-heptadiene (1,6-HPD), which provides highly stereoregular 1,3-*cis-isotactic* (1,3-*c-iso*) poly(1,3-methylenecyclohexane) (PMCH;  $n = 1$  in Chart 1). We further document that the undesirable crystalline properties of these 1,3-*c-iso*-PMCH materials, which are associated with a high  $T_m$  ( $>200$  °C) and slow crystallization kinetics, can be ameliorated while preserving a desirable high  $T_g$  of  $100$  °C through a two-state LCP process that from a single initiator generates a spectrum of different *isotactic stereoblock* forms with decreasing stereoblock length in a programmed fashion (Scheme 1). Finally, we present preliminary evidence to show that this stereoengineering strategy can be used to manipulate the solid-state microphase-separated morphology of PMCH-*b*-PH [PH = poly(1-hexene)] block copolymers.

In contrast to the well-established and growing body of work detailing the coordination polymerization of 1,5-HXD and PMCP,<sup>6–8</sup> little is known about the analogous polymerization of 1,6-HPD to provide structurally coherent PMCH.<sup>11</sup> Indeed, to

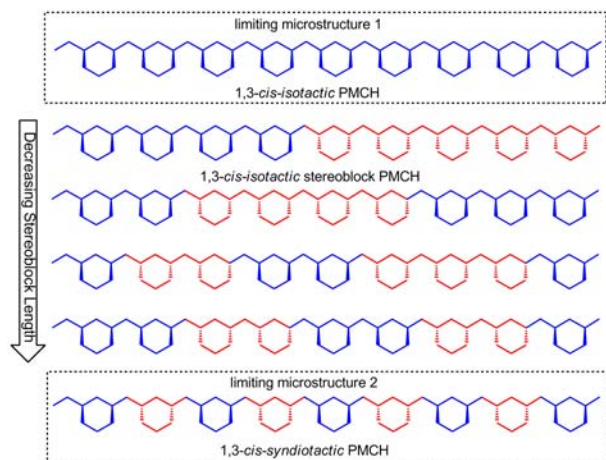
Chart 1



Received: March 4, 2013

Published: May 22, 2013

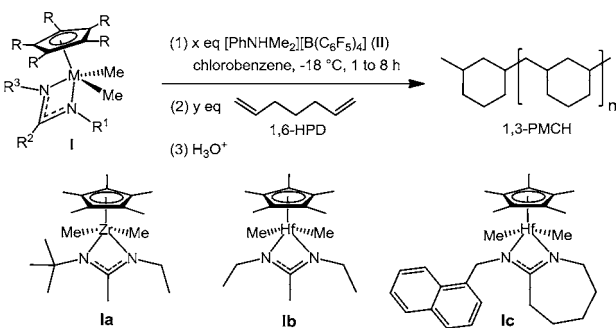
Scheme 1



the best of our knowledge, PMCH has only been briefly described twice before.<sup>7b,9</sup> Most notably, Edson and Coates<sup>9</sup> reported the use of a Hf complex as the catalyst for nonliving stereoselective polymerization of 1,6-HPD to provide a low yield of highly stereoregular 1,3-*c-iso*-PMCH that displayed enigmatic solid-state thermal phase behavior: namely, a reproducible  $T_g$  of 103.9 °C but a transient  $T_m$  of 179.0 °C that was observed only in the first heat/cool cycle in a differential scanning calorimetry (DSC) analysis.

In the present study, a preliminary screen of the LCP of 1,6-HPD using the derivatives **1a**,<sup>12</sup> **1b**,<sup>13</sup> and **1c**<sup>14</sup> was conducted (Scheme 2), and gratifyingly, nearly quantitative yields of the

Scheme 2



respective PMCH products **1a–c** were obtained [Table 1 in the Supporting Information (SI)].<sup>15</sup> Support for the living character of these polymerizations was established by routine methods, including gel-permeation chromatography analyses that yielded monomodal and very narrow molecular weight distributions, as indicated by the low values ( $\leq 1.1$ ) of the polydispersity index ( $D = M_w/M_n$ , where  $M_n$  and  $M_w$  are the number-average and weight-average molecular weights, respectively). <sup>1</sup>H NMR spectra [600 MHz, 1,1,2,2-tetrachloroethane-*d*<sub>2</sub> (TCE-*d*<sub>2</sub>), 110 °C] also confirmed the absence of vinylic end-group resonances that might arise from irreversible chain termination of the propagating species through  $\beta$ -hydrogen transfer processes as well as the complete absence of resonances for pendant side-chain vinyl groups due to the regiospecific cyclopolymerization of 1,6-HPD during chain growth. This latter observation is significant for the future goal of obtaining more architecturally complex PMCH structures (e.g., block and star copolymers), as it eliminates any concern about cross-linking of polymer chains

during propagation by the living (but starving) polymeryl active species once all of the 1,6-HPD monomer has been completely consumed.

The observed differences in the bulk properties of the PMCH samples were suggestive of variations in the stereochemical microstructure, and this suspicion was confirmed upon comparison of their <sup>13</sup>C{<sup>1</sup>H} NMR spectra (Figure 1). More

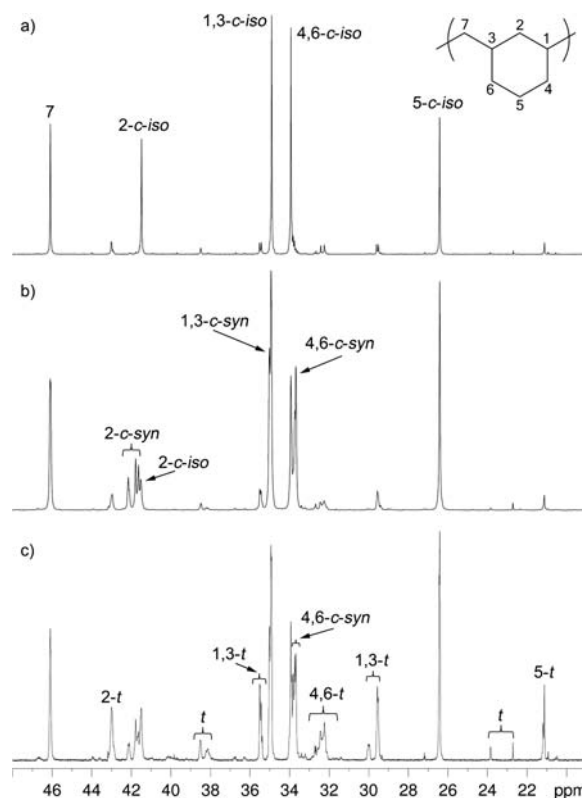


**Figure 1.** <sup>13</sup>C{<sup>1</sup>H} NMR spectra (150 MHz, TCE-*d*<sub>2</sub>, 110 °C) of PMCH materials: (a) **1a**; (b) **1b**; (c) **1c**. Assignments of <sup>13</sup>C resonances are based on the stereochemical microstructures presented in Chart 1 and literature precedent.<sup>9,15</sup>

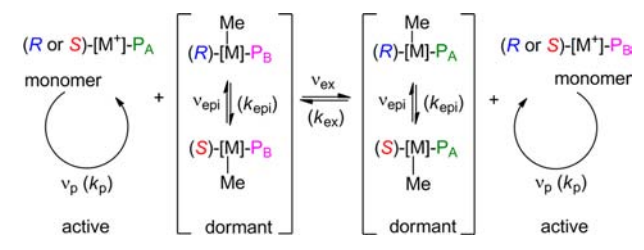
specifically, with  $C_1$ -symmetric **1a**, stereoselective LCP of 1,6-HPD occurred, providing **1a** with an extremely high degree of 1,3-*c-iso* stereoregularity (Figure 1a). On the other hand,  $C_s$ -symmetric **1b** yielded **1b** with a very high degree of 1,3-*cis* selectivity coupled with a low level of stereosequence regularity (Figure 1b), and rather surprisingly, the active species derived from  $C_1$ -symmetric **1c** apparently propagated with virtually no degree of stereocontrol, as evidenced by both the low 1,3-*cis*/1,3-*trans* selectivity and the low stereoregularity (Figure 1c).

Having a sample of highly stereoregular 1,3-*c-iso*-PMCH in hand provided an opportunity to reinvestigate the thermal phase behavior of this material.<sup>15</sup> In brief, DSC analysis of **1a** using a standard heat/cool/heat cycle over the temperature range 50–250 °C at 10 °C/min reproduced the phenomenological observations described by Edson and Coates.<sup>9</sup> However, the high  $T_g$  value of 95 °C indicated that rapid cooling from the melt coupled with intrinsically slow crystallization kinetics produced **1a** in an amorphous glassy state.<sup>16</sup> This conclusion was confirmed by repeating the DSC analysis of **1a** using the same temperature cycle as before but with a greatly attenuated rate of 1 °C/min, which provided reproducible  $T_g$  and  $T_m$  values of 92.2 and 208.5 °C, respectively.<sup>15</sup> On the other hand, this more

extensive DSC study of **1a** also confirmed that the bulk properties of stereoregular 1,3-*c-iso*-PMCH are highly dependent upon the exact thermal history of the material; although this dependency is of scientific interest, it does not bode well for the adoption of this material in technological applications requiring a kinetically stable solid state after processing.<sup>16</sup>

We previously showed that stereoengineering of the stereochemical microstructure of poly( $\alpha$ -olefin)s can be achieved using a “two-state” LCP system in which rapid and reversible methyl group exchange between cationic, configurationally stable active species and neutral, configurationally unstable dormant species is competitive with chain-growth propagation (Scheme 3).<sup>2,17</sup>

Scheme 3



Under the conditions  $\nu_{\text{epi}} > \nu_{\text{ex}} \gg \nu_p$ , where  $\nu_{\text{epi}}$ ,  $\nu_{\text{ex}}$ , and  $\nu_p$  are the rates of metal-centered epimerization of a  $C_1$ -symmetric (chiral) dormant species, methyl group exchange between active and dormant species, and chain-growth propagation of the active species, respectively, the frequency of incorporation of  $(m)_xmr(m)_y$  stereosequences (e.g., *mmrm* pentad and *mmmrmm* heptad) within the growing polymer chain during *isotactic* propagation of an acyclic  $\alpha$ -olefin monomer is proportional to the concentration of dormant states at any given time.<sup>18</sup> Importantly, since the initial concentrations of active and dormant states can be easily set at the start of the two-state LCP in Scheme 3 (vide infra), external control over the rate of exchange between the two populations can be used to generate in a programmed fashion a spectrum of different physical variants of the poly( $\alpha$ -olefin) that are defined and constrained within two limiting microstructural forms (e.g., *isotactic* and *atactic*). In this manner, the programmed synthesis of a well-defined *isotactic/atactic* stereogradient and stereoblock polypropylene thermoplastic elastomers of configurable stereoblock length, linear sequence, and architecture (e.g., di-, tri-, or tetrablock) was achieved.<sup>17c-e</sup>

Because of the increased level of structural complexity that arises when two different stereochemistry-defining events occur during chain-growth propagation of an  $\alpha,\omega$ -nonconjugated diene, it was not a given that PMCHs would be amenable to the same stereoengineering strategy. Thus, we first validated that the mechanism of Scheme 3 could be used to manipulate the stereochemical microstructure of 1,3-*c-iso*-PMCH by performing a series of LCPs of 1,6-HPD in which decreasing **II:Ia** ratios were used to establish an increasing initial concentration of dormant states.<sup>15</sup> The  $^{13}\text{C}\{^1\text{H}\}$  NMR spectra for **1a** (obtained by 100% “activation” of **Ia** by **II**), **1d** (90%), **1e** (80%), and **1f** (50%) clearly showed a steady change from the highly stereoregular microstructure of **1a** with increasing dormant state concentration (Figure 2). It is important to stress here that in all cases the propagation remained highly 1,3-*c-iso*-selective, but as the dormant state concentration increased, the probability for metal-centered epimerization of a dormant state to occur after cycloinsertion of a 1,6-HPD monomer into the growing PMCH

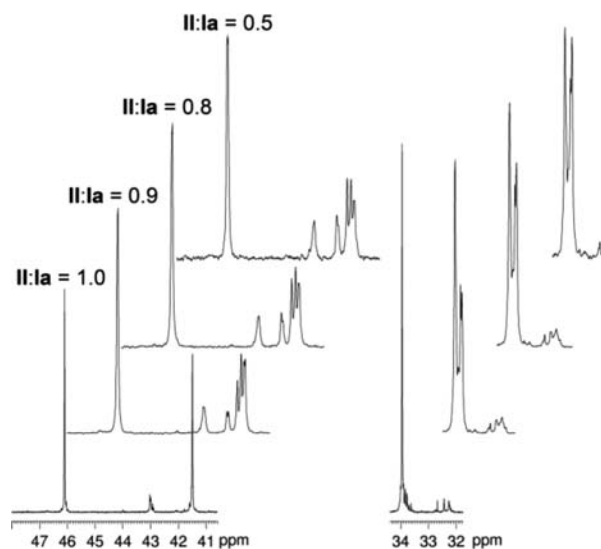


**Figure 2.** Partial  $^{13}\text{C}\{^1\text{H}\}$  NMR spectra (150 MHz, TCE- $d_2$ , 110 °C) of PMCH materials obtained using different **II:Ia** ratios. Stacked spectra (successively right-shifted by 2 ppm for clarity) are shown for (bottom to top) **1a** (100% activation of **Ia** by **II**), **1d** (90%), **1e** (80%), and **1f** (50%). Spectra for **1g** (95%), **1h** (87%), **1i** (85%), and **1j** (75%) are presented in the SI.<sup>15</sup>

chain also increased. At the stereochemical microstructure level, the mechanism of Scheme 3 dictates that an *isotactic stereoblock* relationship exists for the PMCH materials in Figure 2, with the stereoblock length steadily decreasing in the order **1d** > **1e** > **1f**, as illustrated in Scheme 1. The products **1g** (95% activation), **1h** (87%), **1i** (85%), and **1j** (75%) also gratifyingly provided  $^{13}\text{C}$  NMR spectra in keeping with this conclusion.<sup>15</sup> Finally, while DSC and wide-angle X-ray diffraction (WAXD) analyses of **1a** and **1g** confirmed them to be semicrystalline materials, the other members of the set (**1b–f** and **1h–j**) all were unequivocally amorphous, with no observable  $T_m$  arising under a variety of thermal annealing conditions. On the other hand, and most significantly, this latter group of 1,3-*c-iso*-PMCH materials all displayed nearly identical and reproducible high  $T_g$  values of 92–98 °C, as established by DSC.<sup>15</sup>

To determine whether the differences in the stereochemical microstructures and bulk properties of the set of stereoengineered 1,3-*c-iso*-PMCH homopolymers would be manifested as observables within a corresponding set of PMCH-based block copolymers, sequential LCPs of fixed amounts of 1,6-HPD and 1-hexene with **Ia** at 100% and 50% activation were used to prepare the PMCH-*b*-PH diblock copolymers **2a** ( $M_n = 28.6$  kDa,  $D = 1.15$ ) and **2b** ( $M_n = 25.2$  kDa,  $D = 1.04$ ).<sup>15</sup>  $^1\text{H}$  NMR spectra established that the relative PMCH fractions in these diblock copolymers were 0.29 and 0.25, respectively, and  $^{13}\text{C}$  NMR spectra further confirmed that, as expected, the 1,3-*c-iso*-PMCH and *iso*-PH blocks of **2a** were highly stereoregular, whereas the PMCH block microstructure of **2b** resembled that of **1f** and the PH block of this material appeared to be stereorandom (i.e., *atactic*).

The surface morphologies of thermally annealed 160 nm thick films of **2a** and **2b** were visualized using phase-sensitive tapping-mode atomic force microscopy (ps-tm-AFM).<sup>15,19</sup> In the phase maps (Figure 3), both **2a** and **2b** appear to adopt a microphase-separated cylindrical morphology;<sup>8,20</sup> however, a distinct difference between the two is quite noticeable, as the distance over which a particular surface-parallel PMCH cylindrical domain

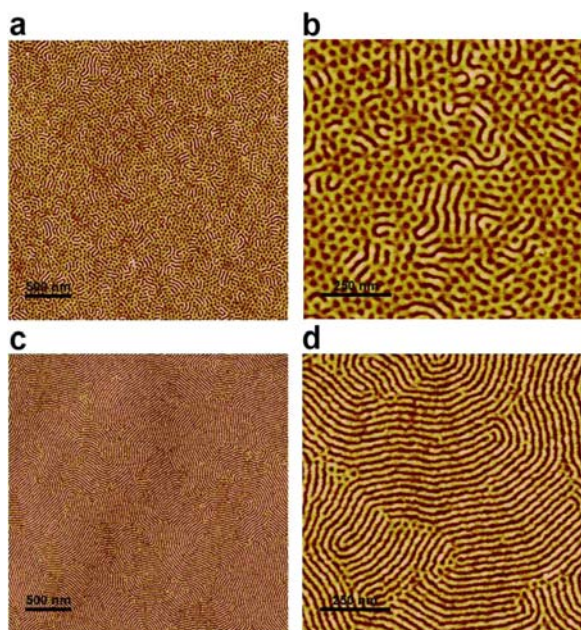


**Figure 3.** ps-tm-AFM phase maps of thermally annealed 160 nm thick films of (a, b) **2a** and (c, d) **2b**.<sup>15</sup>

extends is much greater for **2b** than for **2a**. Although more detailed solid-state structural studies are required, a reasonable conjecture is that the highly stereoregular microstructure of 1,3-*c*-iso-PMCH in **2a** contributes to a greater barrier for establishing efficient long-range PMCH domain chain packing vis-à-vis **2b**.<sup>20,21</sup>

In conclusion, the preliminary results presented herein serve to expand the utility of a two-state LCP process for stereo-engineering of the stereochemical microstructure of PMCH, which in turn may now provide access to new material science and applications involving this novel class of polyolefins possessing high  $T_g$ .

## ■ ASSOCIATED CONTENT

### Supporting Information

Experimental details. This material is available free of charge via the Internet at <http://pubs.acs.org>.

## ■ AUTHOR INFORMATION

### Corresponding Author

lsita@umd.edu

### Notes

The authors declare no competing financial interest.

## ■ ACKNOWLEDGMENTS

We thank the NSF (CHE-1152294) for funding and acknowledge Mr. Wonseok Hwang for WAXD characterization and helpful discussions regarding ps-tm-AFM.

## ■ REFERENCES

- (1) Edson, J. B.; Domski, G. J.; Rose, J. M.; Bolig, A. D.; Brookhart, M.; Coates, G. W. In *Controlled and Living Polymerizations: From Mechanisms to Applications*; Mueller, A. H. E., Matyjaszewski, K., Eds.; Wiley-VCH: Weinheim, Germany, 2009; p 167.
- (2) Sita, L. R. *Angew. Chem., Int. Ed.* **2009**, *48*, 2464.
- (3) (a) White, J. L.; Choi, D. D. *Polyolefins: Processing, Structure Development, and Properties*, 1st ed.; Hanser: Cincinnati, OH, 2004; p 18.

(b) Sperling, L. H. *Introduction to Physical Polymer Science*, 4th ed.; Wiley: Hoboken, NJ, 2006; p 411.

(4) Atactic poly(vinylcyclohexane) (PVCH) has  $T_g = 80^\circ\text{C}$ , whereas isotactic PVCH has  $T_g = 165^\circ\text{C}$  and  $T_m > 400^\circ\text{C}$ . See: Grebowicz, J. S. *Polym. Eng. Sci.* **1992**, *32*, 1228.

(5) Kim, I. In *Stereoselective Polymerization with Single-Site Catalysts*; Baugh, L. S., Canich, J. A. M., Eds.; CRC Press: Boca Raton, FL, 2008; p 489.

(6) (a) Resconi, L.; Waymouth, R. M. *J. Am. Chem. Soc.* **1990**, *112*, 4953. (b) Resconi, L.; Coates, G. W.; Mogstad, A.; Waymouth, R. M. *J. Macromol. Sci., Chem.* **1991**, *A28*, 1225. (c) Cavallo, L.; Guerra, G.; Corradini, P.; Resconi, L.; Waymouth, R. M. *Macromolecules* **1993**, *26*, 260. (d) Schaverien, C. J. *Organometallics* **1994**, *13*, 69. (e) Jeremic, D.; Wang, Q. Y.; Quyoum, R.; Baird, M. C. *J. Organomet. Chem.* **1995**, *497*, 143. (f) Mitani, M.; Oouchi, K.; Hayakawa, M.; Yamada, T.; Mukaiyama, T. *Chem. Lett.* **1995**, *24*, 905. (g) Kim, I. L.; Shin, Y. S.; Lee, J. K.; Won, M. S. *J. Polym. Sci., Part A: Polym. Chem.* **2000**, *38*, 1520. (h) Hustad, P. D.; Coates, G. W. *J. Am. Chem. Soc.* **2002**, *124*, 11578. (i) Yeori, A.; Goldberg, I.; Schuster, M.; Kol, M. *J. Am. Chem. Soc.* **2006**, *128*, 13062. (j) Volkis, V.; Averbuj, C.; Eisen, M. S. *J. Organomet. Chem.* **2007**, *692*, 1940. (k) Shi, X.; Wang, Y.; Liu, J.; Cui, D.; Men, Y.; Li, Y. *Macromolecules* **2011**, *44*, 1062.

(7) (a) Coates, G. W.; Waymouth, R. M. *J. Am. Chem. Soc.* **1991**, *113*, 6270. (b) Coates, G. W.; Waymouth, R. M. *J. Mol. Catal.* **1992**, *76*, 189. (c) Coates, G. W.; Waymouth, R. M. *J. Am. Chem. Soc.* **1993**, *115*, 91. (d) Yeori, A.; Goldberg, I.; Kol, M. *Macromolecules* **2007**, *40*, 8521. (e) Naga, N.; Yabe, T.; Sawaguchi, A.; Sone, M.; Noguchi, K.; Murase, S. *Macromolecules* **2008**, *41*, 7448. (f) Naga, N.; Shimura, H.; Sone, M. *Macromolecules* **2009**, *42*, 7631.

(8) Jayaratne, K. C.; Keaton, R. J.; Henningsen, D. A.; Sita, L. R. *J. Am. Chem. Soc.* **2000**, *122*, 10490.

(9) Edson, J. B.; Coates, G. W. *Macromol. Rapid Commun.* **2009**, *30*, 1900.

(10) Naga, N.; Shiono, T.; Ikeda, T. *Macromol. Chem. Phys.* **1999**, 1466.

(11) Competitive 1,2- vs 2,1-regioselectivity in ring-closing insertion or isomerization/polymerization that occurs in the case of some late-transition-metal catalysts provides polyolefins that are structurally distinct from PMCAs. For example, see: (a) Takeuchi, D.; Matsuura, R.; Park, S.; Osakada, K. *J. Am. Chem. Soc.* **2007**, *129*, 7002. (b) Takeuchi, D.; Osakada, K. *Polymer* **2008**, *49*, 4911.

(12) Jayaratne, K. C.; Sita, L. R. *J. Am. Chem. Soc.* **2000**, *122*, 958.

(13) Zhang, W.; Sita, L. R. *J. Am. Chem. Soc.* **2008**, *130*, 442.

(14) Sita, L. R.; Wei, J.; Yonke, B. L.; Redman, D. W. To be submitted.

(15) Experimental details are provided in the SI.

(16) For example, see: Di Lorenzo, M. L.; Righetti, M. C.; Wunderlich, B. *Macromolecules* **2009**, *42*, 9312.

(17) (a) Zhang, Y.; Keaton, R. J.; Sita, L. R. *J. Am. Chem. Soc.* **2003**, *125*, 9062. (b) Zhang, Y.; Sita, L. R. *J. Am. Chem. Soc.* **2004**, *126*, 7776.

(c) Harney, M. B.; Zhang, Y.; Sita, L. R. *Angew. Chem., Int. Ed.* **2006**, *45*, 2400. (d) Harney, M. B.; Zhang, Y.; Sita, L. R. *Angew. Chem., Int. Ed.* **2006**, *45*, 6140. (e) Giller, C.; Gururajan, G.; Wei, J.; Zhang, W.; Hwang, W.; Chase, D. B.; Rabolt, J. F.; Sita, L. R. *Macromolecules* **2011**, *44*, 471.

(18) For  $\nu_{ex}(k_{ex}) \gg \nu_p(k_p)$ , active and dormant sites effectively propagate at the same rate, and all of the desired characteristics of a living polymerization can be maintained, including control over the number-average degree of polymerization,  $X_n = \{[\text{monomer}]_t - [\text{monomer}]_0\} / \{[\text{active}]_0 + [\text{dormant}]_0\}$ .

(19) (a) van Dijk, M. A.; van den Berg, R. *Macromolecules* **1995**, *28*, 6773. (b) Stocker, W.; Beckmann, J.; Stadler, R.; Rabe, J. P. *Macromolecules* **1996**, *29*, 7502. (c) Leclère, P.; Lazzaroni, R.; Brédas, J. L.; Yu, J. M.; Dubois, P.; Jérôme, R. *Langmuir* **1996**, *12*, 4317. (d) Hobbs, J. K.; Register, R. A. *Macromolecules* **2006**, *39*, 703.

(20) (a) Hamley, I. W. *The Physics of Block Copolymers*; Oxford University Press: New York, 1998. (b) Loo, Y.-L.; Register, R. A. In *Developments in Block Copolymer Science and Technology*; Hamley, I. W., Ed.; Wiley: Chichester, U.K., 2004; pp 213–243.

(21) DSC and WAXD characterization of **2a** did not provide conclusive evidence of PMCH domain crystallinity.